



Extraction of trace polychlorinated biphenyls in environmental waters by well-dispersed velvet-like magnetic carbon nitride nanocomposites



Dandan Li^{a,1}, Jun Zhu^{a,1}, Man Wang^a, Wentao Bi^{a,*}, Xiaohua Huang^a, David Da Yong Chen^{a,b,**}

^a Jiangsu Collaborative Innovation Center of Biomedical Functional Materials, Jiangsu Key Laboratory of Biomedical Materials, College of Chemistry and Materials Science, Nanjing Normal University, Nanjing 210023, China

^b Department of Chemistry, University of British Columbia, Vancouver, BC V6T 1Z1, Canada

ARTICLE INFO

Article history:

Received 20 February 2017

Accepted 21 February 2017

Available online 22 February 2017

Keywords:

Magnetic solid phase extraction

Polychlorinated biphenyls

Velvet-like carbon nitride

Rapid adsorption and desorption

ABSTRACT

A velvet-like magnetic carbon nitride nanocomposites synthesized by chemical co-precipitation was used to develop a highly efficient magnetic solid-phase extraction method for the pre-concentration of trace polychlorinated biphenyls (PCBs) in water samples. The advantages of this nanocomposite such as large surface area, good dispersity, low solvent consumption, rapid analyte adsorption (30 s) and reusability make it a good sorbent. Factors affecting extraction efficiency were systematically investigated and optimized by response surface methodology (RSM). Under optimal experimental conditions, the limits of detection (LODs S/N=3) of the developed method for PCBs investigated were in the range of 9.0×10^{-6} – 5.8×10^{-5} $\mu\text{g/mL}$. This method was then used for the analysis of four real water samples. Good spiked recoveries over the range of 80.1–118.4%, and RSDs ($n=5$) of 0.02–3.7% were obtained. This work demonstrated the potential of using this nanocomposite for adsorption, pre-concentration, or even removal of different carbon-based aromatic compounds or other hydrophobic pollutants.

© 2017 Elsevier B.V. All rights reserved.

1. Introduction

Industrial, agricultural and domestically released pollutants often cause significant concerns by the general public. The monitoring of these environmental pollutants is essential in the effort to limiting the adverse effects of these compounds on human health [1–5]. Due to their trace concentration in water environments, it is vital to develop efficient analytical techniques to analyze the ultra-trace amount of compounds. Usually one or more pre-treatment step is needed for pre-concentration for analysis and multiple steps are required to eliminate them. Traditional sample pretreatment methods such as liquid–liquid extraction (LLE) [6], solid phase

extraction (SPE) [7], membrane extraction, dispersive solid-phase extraction (DSPE) [8], liquid phase microextraction (LPME) [9] and solid phase microextraction (SPME) [10]. Solid phase extraction (SPE) is a widely used sample pretreatment method for separation, purification and enrichment [11]. However, SPE still has disadvantages such as time-consuming, high solvent consumption, and low recovery [12–16]. In order to solve these problems and meet the needs for analysis, methods with wide concentration range, high selectivity and sensitivity are needed. Magnetic solid phase extraction (MSPE) has attracted much attention recently, and has increasingly been developed and used in different areas [17]. MSPE has been used in sample separation and concentration in the field of food industry, biology and environmental sciences because of the advantages of easy operation, high-adsorption capacity and short operation time. Magnetic adsorbents need not be filled in SPE cartridges, but instead, can be dispersed in the sample solution or suspension, and is suitable for many types of sample matrices even when the sample is non-homogeneous. Unlike the traditional SPE technology, the organic compounds are adsorbed by the magnetic material, separated from the solution by using external magnetic field instead of centrifugation or filtration, and eluted by a small volume of proper eluent from the sorbent in MSPE [18].

* Corresponding author at: Jiangsu Collaborative Innovation Center of Biomedical Functional Materials, Jiangsu Key Laboratory of Biomedical Materials, College of Chemistry and Materials Science, Nanjing Normal University, Nanjing 210023, China

** Corresponding author at: Department of Chemistry, University of British Columbia, Vancouver, BC V6T 1Z1, Canada.

E-mail addresses: biwentao@njnu.edu.cn (W. Bi), chen@chem.ubc.ca (D.D.Y. Chen).

¹ These authors contributed equally to this work.

It is crucial to select appropriate sorbent to achieve efficient extraction in SPE, and this is also true for magnetic adsorbent in MSPE. It is important to prepare the magnetic sorbent with high adsorption capacity for the target compounds. Recently, a two-dimensional graphite analogue, graphitic carbon nitride that is referred to as $g\text{-C}_3\text{N}_4$ has attracted much attention, and is a possible candidate to be used for enrichment of target analytes in solutions. $g\text{-C}_3\text{N}_4$ is the most stable allotrope under ambient conditions among the family of carbon nitrides, and is thermally stable up to 500°C [19]. Furthermore, it is only composed of very common elements, C, N, and H, which also possesses high resistance to acids and bases. It is easily formed by heating of low cost nitrogen-rich organic compounds, such as melamine. Moreover, the simple 2D structure of $g\text{-C}_3\text{N}_4$ can easily swell and peel off into nearly transparent ultrathin nanosheets by aqueous ultrasonication [20,21]. The $g\text{-C}_3\text{N}_4$ sheets have a double-sided polyaromatic scaffold structure with a large π -electron system that equipped it with complex sorption mechanism, including hydrophobic effect, $\pi-\pi$ conjugation and electrostatic interaction [22,23]. This structure provides it with a strong affinity for aromatic compounds that are commonly present in food, drugs, biological fluids and pollutants. Moreover, the simple structure of $g\text{-C}_3\text{N}_4$ allows rapid adsorption and desorption, which reduced the processing time, solvent consumption, and increased recovery. These unique properties highlight its potential for use as a sorbent, but the small specific surface area of this material limited its range of application. The surface area of bulk $g\text{-C}_3\text{N}_4$ is usually less than $5\text{ m}^2/\text{g}$ when synthesised by the traditional thermal condensation method. Many forms of nanoscale structures of $g\text{-C}_3\text{N}_4$, such as nanoparticles, nanosheets, nanofibers, nanopores and nanotubes have been synthesised to increase the specific surface area and produce more accessible sites. Nevertheless, these synthetic methods largely depend on the use of hard or soft templates, special instruments and complicated processes. Therefore, it is highly desirable to develop a simple and facile approach for the synthesis of $g\text{-C}_3\text{N}_4$ with a large specific surface area for practical applications. Attempts towards this goal have led to the synthesis of various forms of $g\text{-C}_3\text{N}_4$, including a velvet-like $g\text{-C}_3\text{N}_4$ (V- $g\text{-C}_3\text{N}_4$) via a water-assisted, one-step thermal condensation of urea. In the process of synthesis, it was free of templates, toxic solvents and expensive chemicals [21]. To use this synthesized material for MSPE, Fe_3O_4 particles were immobilized on the surface of the V- $g\text{-C}_3\text{N}_4$ [24–26]. In addition, V- $g\text{-C}_3\text{N}_4/\text{Fe}_3\text{O}_4$ has many advantages, such as the large surface area, good dispersity, and strong hydrophobicity. Ten polychlorinated biphenyl (PCBs) were selected as model compounds to evaluate the performance of this magnetic nanocomposite as a sorbent.

PCBs are a group of chlorinated aromatic compound and have different homologs and isomers [27,28]. PCBs are one of the typical persistent organic pollutants in the priority control by Stockholm Convention, due to their high potential of bioaccumulation and resistance to degradation [29]. These pollutants have some characteristics such as biodegradable, biological toxicity, and long-range transportability [30,31]. In addition, PCBs have stable physical and chemical properties and they are semi-volatile or non-volatile matter that has strong causticity. PCBs are still detectable in most environmental matrices, although their use has been legally banned [32,33]. Thus, detecting trace levels of PCBs in the environment is important. In addition, developing efficient and fast analytical methods which are for the determination of PCBs in environmental samples is very important to protect humans from exposure [34]. Therefore ten PCBs (1,3,4,8,28,52,77,126,138 and 180) were chosen as model compounds to demonstrate the feasibility of this V- $g\text{-C}_3\text{N}_4/\text{Fe}_3\text{O}_4$ nanocomposite for the extraction and pre-concentration of PCBs from water samples. Response surface methodology (RSM) was used as the optimization approach to predict the optimized multiple parameters as well as their interactions

by establishing an efficient mathematical model [35–43], according to Box–Behnken Design (BBD). A fast, selective and sensitive method using MSPE and gas chromatography-mass spectrometry (GC–MS) was developed to analyze the ten PCBs in real water samples. And the linearity and the limits of detection (LODs $S/N=3$) of the developed method for PCBs investigated were established by GC/MS.

2. Experimental

2.1. Chemicals

Urea (>99.0%), Ferric chloride hexahydrate (>97.0%), ferrous chloride tetrahydrate (>98.0%), 2-Chlorobiphenyl (PCB-1), 4-Chlorobiphenyl (PCB-3), 2, 2'-Dichlorobiphenyl (PCB-4), 2, 4'-Dichlorobiphenyl (PCB-8), 2,4,4'-Trichlorobiphenyl (PCB-28), 2,2',5,5'-Tetrachlorobiphenyl (PCB-52), 3,3',4,4'-Tetrachlorobiphenyl (PCB-77), 3,3',4,4',5-Pentachlorobiphenyl (PCB-126) 2,2',3,4,4',5'-Hexachlorobiphenyl (PCB-138), and 2,2',3,4,4',5,5'-Heptachlorobiphenyl (PCB-180) were purchased from Aladdin Industrial Inc. (Shanghai, China). Distilled water was filtered using a vacuum pump (Division of Millipore, USA) and a filter (HA-0.45, Division of Millipore, USA) before use. All other solvents were of HPLC or analytical grade.

2.2. Preparation of the standard stock solution

A mixture of PCBs (1,3,4,8,28,52,77,126,138 and 180) containing $100\text{ }\mu\text{g}/\text{mL}$ of each compound was prepared in methanol and stored at 4.0°C . The working solutions were prepared daily by diluting the stock solutions with deionized (DI) water.

2.3. Preparation of V- $g\text{-C}_3\text{N}_4/\text{Fe}_3\text{O}_4$ nanoparticles

According to a typical procedure [21], 15 g of urea was added to 20 mL of de-ionized water in an alumina crucible. Next the V- $g\text{-C}_3\text{N}_4$ was prepared by directly heating urea at 400°C for 1 h, then at 450°C for 5 h in a muffle furnace. Then the product was collected and dried at room temperature. A 2:1 ratio of $\text{FeCl}_3\cdot 6\text{H}_2\text{O}$ (11.68 g) and $\text{FeCl}_2\cdot 4\text{H}_2\text{O}$ (4.30 g) was added to 200 mL deionized water at 85°C , then stir for 5 min. And then gradually adding 20 mL ammonia (25–28%), allow reaction to proceed for two hours. The obtained Fe_3O_4 nanoparticles were washed using water and ethanol then dried in the air.

The V- $g\text{-C}_3\text{N}_4/\text{Fe}_3\text{O}_4$ nanocomposites were obtained by chemical co-precipitation. In a typical synthesis, firstly, V- $g\text{-C}_3\text{N}_4$ (100.0 mg) and Fe_3O_4 (50.0 mg) were dispersed in 60.0 mL of water that ultrasonicated for 0.5 h at room temperature. Secondly, the resulting mixture was stirred at 60°C for 10 h. Finally, the reaction mixture was cooled and washed several times with de-ionized water and ethanol. After that, the synthetic nanocomposite was dried at 60°C in the oven.

2.4. Analysis and characterization

The high performance liquid chromatography (HPLC) system consisted of a Waters 1525 binary HPLC pump, Waters 2707 auto sampler (20.0 μL sample loop), and variable wavelength 2489 ultraviolet (UV) dual channel detector. Data processing was performed with a Millennium 3.2 consisting of a HP Vectra 500PC. A commercial C_{18} column (4.6 \times 150 mm, 5.0 μm) was purchased from Thermo Fisher Scientific Inc., which was used for the separation of target PCBs. The mobile phase was methanol/water (85/15, v/v) at a flow rate of 1.0 mL/min, and UV detection was performed at 235 and 254 nm. The HPLC was used to optimize the sample preparation steps because of the solvent compatibility.

Table 1
Variables and levels of response surface methodology test.

Variables	Level		
	−1	0	1
Concentration of NaCl (X_1) (% w/v)	5.00	10.00	15.00
Temperature (X_2) (°C)	25.00	30.00	35.00

GC–MS analysis was performed on an Agilent 7890B/5977A GC/MS detector system with Split/Splitless with electronic pneumatics control (EPC) and 7693A Autoinjector module. And the MS (5977A) included inert MSD Turbo EI Bundle. MSD Chemstation Software was used for data acquisition and analysis. Analytes were separated on a HP-5 MS (30m × 0.25 mm, 0.25 μm, Agilent) column. The injection volume was 1 μL and Helium (purity 99.995%) was used as carrier gas at a constant flow rate of 1 mL min^{−1}. The oven temperature was programmed as follows: start at 70 °C for 2 min, increase the temperature at a rate of 15 °C/min to 180 °C, holds the temperature for 10 min, then increases at 5 °C/min to 300 °C and held at 300 °C for 10 min. The transfer line, ion source and quadrupole analyzer temperatures were maintained at 300, 230 and 150 °C, respectively. The collision energy was 70 eV. Both the scan and a single ion monitoring (SIM) mode acquisition method with two characteristic ions were selected for the detection of the analytes.

Thermogravimetric measurements were carried out on a NET-ZSCH STA 449 F3 Jupiter simultaneous thermal analyzer at a heating rate of 10 °C/min in oxygen. A Rigaku D/max 2500/PC instrument was employed for X-ray diffraction (XRD) studies. Fourier transform infrared (FT-IR, Bruker Tensor 27) spectra were acquired between 400 and 4000 cm^{−1} at the rate of 20 scans/min using KBr pellets. The transmission electron microscopy (TEM) analysis was performed by a Hitachi H-7650 instrument (Tokyo, Japan). The specific surface area and pore properties of the samples were calculated using the Brunauer–Emmett–Teller (BET) model with nitrogen adsorption–desorption isotherms (N₂ atmosphere at −195.72 °C), which were measured using an ASAP2020 surface area and porosimetry analyzer (Micromeritics, Norcross, GA, USA). The carbon, hydrogen and nitrogen contents of the V-g-C₃N₄ were determined by elemental analysis that performed on an EA1112 (Carlo Erba, Milan, Italy).

2.5. Adsorption of PCBs on V-g-C₃N₄/Fe₃O₄

The nanocomposites (1.0 mg) were added into 1.0 mL of the aqueous standard PCBs solution (1.0 μg/mL of standards were stored in vials) at room temperature. Then, all the mixtures were ultrasonicated until the concentration of the target compounds ceased to decrease and the equilibrium adsorption was obtained. The amounts of PCBs adsorbed on the sorbents were calculated by subtraction. The reproducibility was assessed over three tests.

2.6. Design of RSM for optimization of adsorption parameters

RSM with a two-variable and three-level of Box–Behnken Design (BBD) was employed to optimize the best combination of variables for the adsorbed amounts of four PCBs on V-g-C₃N₄/Fe₃O₄ nanocomposite. The two variables selected for this investigation were X_1 (concentration of NaCl) and X_2 (temperature). The appropriate ranges of the two variables were determined based on single-factor experiments. Three levels of each variable were coded as −1, 0, and +1 (Table 1 and Table S1). Experimental data were fitted to a quadratic polynomial model and the regression coefficient

was obtained. The nonlinear computer-generated quadratic model used in the response surface was as follows:

$$Y = \beta_0 + \sum_{j=1}^k \beta_j X_j + \sum_{j=1}^k \beta_{jj} X_j^2 + \sum_{i < j}^k \beta_{ij} X_i X_j$$

The three-dimensional response surface plots were obtained by Design-Expert[®] 8.0.6 software (Minneapolis, MN, USA) [44,45]. Triplicate analyses were performed at all design points in randomized order. A regression analysis was performed for the experimental data to fit into an empirical second-order polynomial model.

2.7. Procedure of MSPE

As shown in Fig. 1, V-g-C₃N₄/Fe₃O₄ (3.0 mg) was added into 50 mL of the filtrated (0.2 μm) real water sample. NaCl is then added to reach a concentration of 11.3% (w/v), and the temperature is maintained at 33.0 °C, according to the RSM optimized conditions as described in the earlier section. Because of the rapid adsorption, the extraction was carried out for 30 s to ensure that most of the analytes were adsorbed on the solid phase. An external magnet was then used to retain all magnetized sorbent material while the solution is decanted. The sorbent material is then added 1.0 mL ethanol, and again sonicated for 1.0 min. The adsorbed PCBs are washed out in ethanol, and an external magnet is used again while decanting the PCB ethanol solution. The PCB ethanol solution is analyzed with HPLC and GC–MS [46], while the magnetized sorbent is heat dried and ready to be used again.

3. Results and discussion

3.1. Characterization of V-g-C₃N₄/Fe₃O₄

First, element analysis was performed to ascertain the constituents of the samples. The elemental composition results are shown in Table S2. The trace amount of H and O in the V-g-C₃N₄ may ascribe to its NH₂/NH group and the adsorbed CO₂, O₂ and H₂O. The chemical formula is represented as [C₆N₇(NH₂)(NH)]_n [24], which accords with the chemical composition of the prepared g-C₃N₄, C_{2.76}N_{3.57}H_{2.34}. In addition, to quantify the amount of C₃N₄ in the V-g-C₃N₄/Fe₃O₄ composites, thermogravimetric analysis (TGA) was carried out in air from 40 to 800 °C (Fig. S1(a)). It shows the TGA curves for Fe₃O₄, C₃N₄ and V-g-C₃N₄/Fe₃O₄. Gradually, the weight loss beginning at 120 °C can be attributed to the evaporation of water. From 400 °C to 700 °C, approximately 0.36%, 91.16% and 23.81% mass loss was observed for Fe₃O₄, C₃N₄ and V-g-C₃N₄/Fe₃O₄, respectively. It indicates an abrupt weight loss occurred between 400 and 600 °C, because of the oxidation and decomposition of V-g-C₃N₄ in the air. Therefore, the loading of V-g-C₃N₄ on V-g-C₃N₄/Fe₃O₄ was estimated to be ~23 wt%.

XRD were utilized to ascertain the structure of the samples. Fig. S1 (b) displays the XRD patterns of the as prepared V-g-C₃N₄, Fe₃O₄ and V-g-C₃N₄/Fe₃O₄. The XRD patterns of V-g-C₃N₄ sample contain two peaks at about 13.1° and 27.2°, which matches well with the (1 0) and (0 2) crystal planes of V-g-C₃N₄. When the V-g-C₃N₄ was mixed with Fe₃O₄, the diffraction peaks of V-g-C₃N₄ and Fe₃O₄ were weaker than that of pure V-g-C₃N₄ and pure Fe₃O₄, indicating that V-g-C₃N₄/Fe₃O₄ was a two-phase composite composed of V-g-C₃N₄ and Fe₃O₄ [47]. Fig. S1(c) exhibits the FT-IR spectra of V-g-C₃N₄, Fe₃O₄ and V-g-C₃N₄/Fe₃O₄. The bands between 1200 and 1650 cm^{−1} corresponds to the typical stretching modes of CN heterocycles and the characteristic mode of the triazine units (C₆N₇) at 808 cm^{−1} are observed for V-g-C₃N₄, indicating the presence of a typical structure of g-C₃N₄. The broad adsorption band at

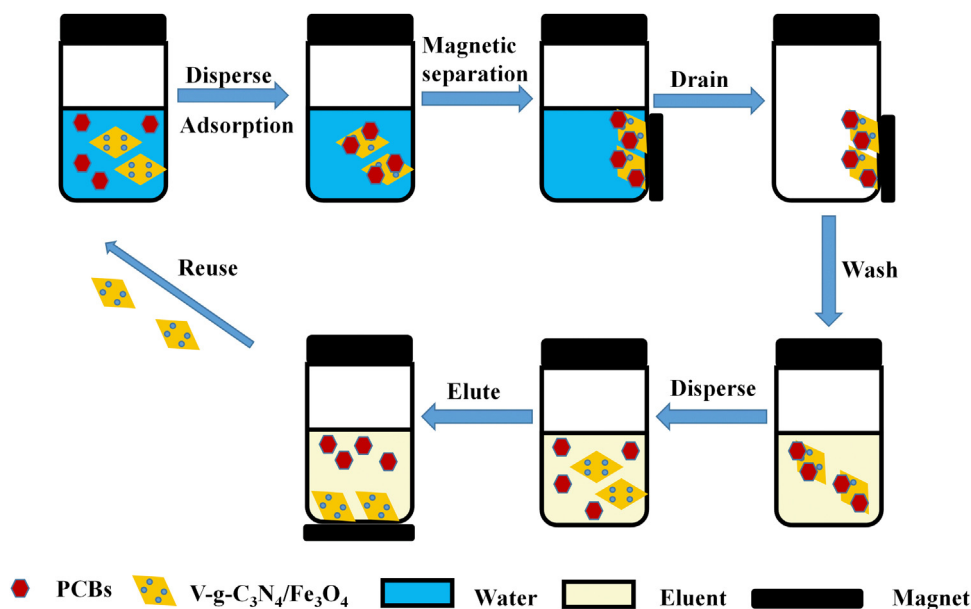


Fig. 1. Process of magnetic solid phase extraction (MSPE).

3100–3300 cm^{-1} corresponded to the stretching vibration modes of residual N–H components or O–H bands, associated with uncondensed amino groups and adsorbed H_2O molecules, respectively. An absorption band at 570 cm^{-1} for both the nanocomposite samples corresponds to the Fe–O band of the Fe_3O_4 particles [48,49]. Above all, the FTIR spectra indicated the successful formation of the V-g- C_3N_4 and V-g- $\text{C}_3\text{N}_4/\text{Fe}_3\text{O}_4$ nanocomposites. To measure the surface areas of these materials, nitrogen adsorption–desorption was employed and the Brunauer–Emmett–Teller (BET) specific surface areas of V-g- C_3N_4 and V-g- $\text{C}_3\text{N}_4/\text{Fe}_3\text{O}_4$ were found to be 151.5 and 126.6 m^2/g (Fig. S1(d)), respectively [50]. The decreased surface area of V-g- $\text{C}_3\text{N}_4/\text{Fe}_3\text{O}_4$ can be attributed to the deposition of Fe_3O_4 on V-g- C_3N_4 . To confirm the deposition and understand the morphologies of V-g- C_3N_4 and V-g- $\text{C}_3\text{N}_4/\text{Fe}_3\text{O}_4$, the two solids were characterized by TEM techniques [51]. As shown in Fig. S2, pure V-g- C_3N_4 consisted of a transparent silk-like structure, whereas in V-g- $\text{C}_3\text{N}_4/\text{Fe}_3\text{O}_4$, dark Fe_3O_4 nanoparticles were deposited on the surface of V-g- C_3N_4 . Three batches of the synthesized nanoparticles were characterized to prove the reproducibility of the synthetic process. No obvious different was observed from the TEM images.

3.2. Optimization of the procedure

To obtain high extraction efficiency for using the V-g- $\text{C}_3\text{N}_4/\text{Fe}_3\text{O}_4$ as sorbent, several factors that influence the adsorption and desorption were investigated. Meanwhile, ultrasonication was employed to suspend the nanocomposite in water samples. The aggregated nanocomposite was disrupted by ultrasonic vibrations leading to an increase in the total solid surface in contact with the water containing the target compounds.

3.2.1. Adsorption isotherms

The initial concentration of PCBs can affect the actual adsorbed amount on the V-g- $\text{C}_3\text{N}_4/\text{Fe}_3\text{O}_4$ nanocomposite. In order to investigate the interactions between PCBs and the nanocomposite as well as choosing the suitable concentration of PCBs for subsequent optimization of MSPE, the adsorption isotherms were introduced. The adsorbed amounts (Q) of PCBs on V-g- $\text{C}_3\text{N}_4/\text{Fe}_3\text{O}_4$ were determined as Eq. (1) and were shown in Fig. 2. All the data were fitted with the following adsorption isotherm models (Eqs. (2)–(4)) [52–54]:

$$Q = (C_0 - C)V/m \quad (1)$$

$$Q = aC_E + b \quad (2)$$

$$Q = aC_E/(1 + bC_E) \quad (3)$$

$$Q = aC_E^{1/c} \quad (4)$$

where Q (mg g^{-1}) is the adsorbed amount, C_0 ($\mu\text{g mL}^{-1}$) is the initiator concentration, C ($\mu\text{g mL}^{-1}$) is the unadsorbed concentration and C_E ($\mu\text{g mL}^{-1}$) is the equilibrium concentration of the solute in the liquid phase. V (mL) is the volume of the sample solvent, and m (g) is the weight of V-g- $\text{C}_3\text{N}_4/\text{Fe}_3\text{O}_4$. In the equations, a and b are the coefficients. These adsorption isotherm equations are linear (Eq. (2)), Langmuir (Eq. (3)) and Freundlich (Eq. (4)) equations, respectively. The Langmuir equation was evidently better than the others in this experiment according to the regression coefficient (R^2) in Table S3. This could be explained by the basic assumptions of Langmuir model: the surface containing the adsorbing sites is a perfectly flat plane with no corrugations; each site can hold at most one molecule (monolayer adsorption).

According to this data, the adsorption of the ten PCBs increased with increasing concentration from 0.1–3.0 $\mu\text{g/mL}$, and the amount of the PCBs adsorbed on the sorbents decreased in the order: PCB-180 > PCB-138 > PCB-126 > PCB-77 > PCB-52 > PCB-28 > PCB-8 > PCB-4 > PCB-3 > PCB-1, which was consistent with their hydrophobicity (Fig. 2). This phenomenon suggested that hydrophobic interaction may be one of the critical interactions between the PCBs and the sorbent, in addition to π – π interactions. To investigate the other effects on the adsorption behavior and to avoid errors in the extraction process, 2.0 $\mu\text{g/mL}$ of PCBs was used in the rest of the experiment.

3.2.2. Optimization of the adsorption conditions by RSM

In MSPE process, single factor experiments were performed to determine the scope of the variables to obtain a more realistic mode before optimization of adsorption by RSM. Firstly, the effect of time on adsorption was investigated between 30 s and 420 s, and shown in Fig. S3 (a). According to the data, time has little effect on adsorption of target compounds. It could be concluded that the adsorption equilibrium between the liquid phase and the sorbent was reached rapidly, before 30 s. This rapid adsorption can be attributed to the good dispersity of V-g- $\text{C}_3\text{N}_4/\text{Fe}_3\text{O}_4$ and strong interactions with target compounds. The effect of salinity was then investigated within the concentration range of 0–25.0% of NaCl (w/v). It can be seen that

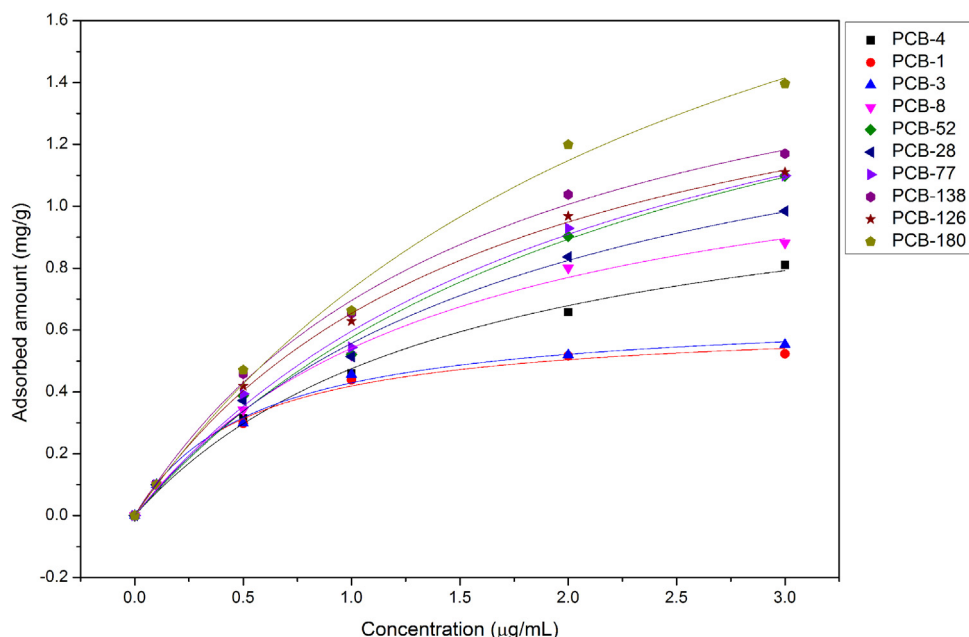


Fig. 2. Adsorbed amount of standard PCBs on V-g-C₃N₄/Fe₃O₄.

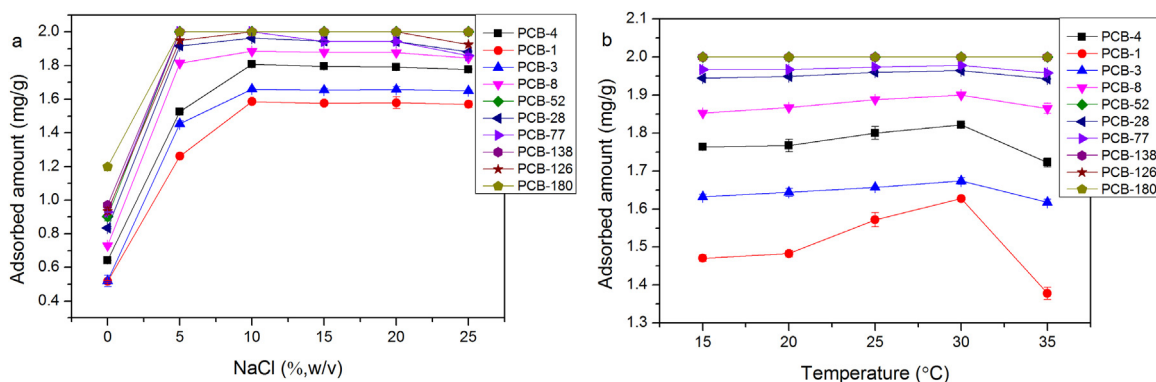


Fig. 3. Effect of concentration of NaCl (a) and temperature (b) on adsorbed amount of PCBs on porous V-g-C₃N₄/Fe₃O₄.

the adsorption of PCBs increased with the addition of NaCl from 0 to 10.0% and then decreased (Fig. 3(a)). Typically, the addition of salts may increase the adsorbed efficiency of target compounds and decrease the solubility of PCBs (salting-out effect). However, this also results in the increase of the viscosity of the solution, which decreased the mass transfer rate and extraction efficiency of PCBs. Therefore, 10.0% of NaCl was added for subsequent optimization. The effect of the solution pH on adsorption was studied in the range of 1.0–11.0 by adding proper volumes of 1 M HCl or 1 M NaOH. The pH of the solution may affect the charge state of the target compounds and their interactions with each other and the sorbent. As shown in Fig. S3 (b) that the pH of the solution also has little effect on adsorption. The reason for this phenomenon could be explained that PCBs are neutral molecules under ordinary conditions and are unlikely to be influenced by a change in the solution pH. The effect of temperature was also investigated because an increase in diffusivity can be achieved by increasing the temperature, and decreasing the solution viscosity, and results in increased adsorption efficiency. However, higher temperature decreased the interactions between target compounds and sorbent resulting in decrease of adsorption. Fig. 3(b) shows that the adsorbed amounts of PCBs increased with the temperature increasing from 15.0 to 30.0 °C and then decreased. Therefore, to optimize the adsorption conditions subsequently by RSM, the ranges of the concentration

of NaCl (5.00–15.00%, w/v) and temperature (25.0–35.0 °C) were selected.

After fitting the experimental data to the quadratic polynomial mode (Table S4), PCB-138 and PCB-180 had been fully adsorbed completely because of their strong hydrophobicity. In addition, an analysis of the variance (ANOVA) indicated that the models were statistically significant, as evidenced from the *F*-test with very low probability values, which were $p < 0.0001$ for PCB-1, PCB-4, and PCB-126, 0.0002 for PCB-3, PCB-8, PCB-28, and PCB-77, and 0.0003 for PCB-52, respectively. The determination coefficients (R^2) of the quadratic polynomial models were 0.9945 for PCB-1, 0.9622 for PCB-3, 0.9929 for PCB-4, 0.9481 for PCB-8, 0.9495 for PCB-28, 0.9453 for PCB-52, 0.9533 for PCB-77, and 0.9642 for PCB-126 with no significant lack of fit (0.0799–0.6564). These showed that the calculated models could be used to explain 94.53–99.45% of the results. The adjusted coefficients of determination ($R^2_{Adj} = 0.9906$ for PCB-1, 0.9352 for PCB-3, 0.9878 for PCB-4, 0.9111 for PCB-8, 0.9134 for PCB-28, 0.9063 for PCB-52, 0.9199 for PCB-77, and 0.9386 for PCB-126), and the coefficient of variation (CV = 0.73 for PCB-1, 0.85 for PCB-3, 0.41 for PCB-4, 0.60 for PCB-8, 0.33 for PCB-28, 0.42 for PCB-77, and 0.37 for PCB-126) suggest that the accuracy and general availability of the polynomial model was adequate. “Adeq Precision” (AP) measures the signal to noise ratio and a ratio greater than 4 is desirable. The ratio of this work (AP = 43.280 for PCB-1,

17.966 for PCB-3, 38.144 for PCB-4, 17.062 for PCB-8, 19.432 for PCB-28, 13.108 for PCB-52, 18.316 for PCB-77, and 19.923 for PCB-126) indicates an adequate signal. Thus, this model can be used to navigate the design space.

The predicted response Y for the adsorbed amount of PCBs could be expressed by the following second-order polynomial equation in term of coded values:

$$Y(\text{PCB-1}) = 1.63 + 0.13X_1 + 0.03X_2 + 0.028X_1X_2 - 0.082X_1^2 - 0.067X_2^2$$

$$Y(\text{PCB-3}) = 1.67 + 0.057X_1 + 0.015X_2 - 5.00 \times 10^{-3}X_1X_2 - 0.042X_1^2 - 0.037X_2^2$$

$$Y(\text{PCB-4}) = 1.82 + 0.072X_1 + 0.022X_2 + 0.02X_1X_2 - 0.047X_1^2 - 0.037X_2^2$$

$$Y(\text{PCB-8}) = 1.89 + 0.037X_1 + 0.028X_2 - 0.021X_1^2 - 0.016X_2^2$$

$$Y(\text{PCB-28}) = 1.96 + 0.01X_1 + 0.022X_2 - 0.0075X_1X_2 - 0.024X_1^2 + 0.001207X_2^2$$

$$Y(\text{PCB-52}) = 2.00 + 3.33 \times 10^{-3}X_2 - 5 \times 10^{-3}X_1X_2 - 0.019X_1^2 - 8.966 \times 10^{-3}X_2^2$$

$$Y(\text{PCB-77}) = 1.99 + 0.001667X_1 + 0.018X_2 - 0.025X_1X_2 - 0.041X_1^2 - 8.62 \times 10^{-4}X_2^2$$

$$Y(\text{PCB-126}) = 2.00 + 0.00667X_1 + 0.033X_2 - 0.0075X_1X_2 - 0.018X_1^2 - 0.018X_2^2$$

where Y represented the adsorbed amount of PCBs (mg g^{-1}), and X_1 and X_2 correspond to two independent variables (concentration of NaCl, and temperature of the solution, respectively). The regression equation was graphically represented by a 3D response surface. From the 3D response surface curves indicated in Fig. S4, it showed visually the effects and mutual influence of two independent variables on the responding variable. According to the p value (Table S5) and the 3D response curves, the significance of each coefficient could be checked. For PCB-28, PCB-52, PCB-77, and PCB-126, the effects of temperature on adsorption were more significant than the concentration of NaCl. On the contrary, the effect of the concentration of NaCl for adsorption of PCB-1, PCB-3, PCB-4 PCB-8 were more significant. This phenomenon could be explained by their different hydrophobicity and molecular size. It is known that the diffusivity significantly affects the adsorption efficiency. It can be studied using the Stokes–Einstein equation:

$$D = kT / 6\pi\eta R$$

where D (area/time) is a proportionality constant between the molar flux owing to molecular diffusion and the gradient in the concentration of the species. k , T , η , and R are the Boltzmann constant, absolute temperature, viscosity of the solution and hydrodynamic radius of the molecule, respectively. According to the equation, the change of temperature can significantly affect the diffusivity of PCB-28, PCB-52, PCB-77, and PCB-126 because of their radius were larger than those of PCB-1, PCB-3, PCB-4, and PCB-8, thus affect the adsorption. Compared to PCB-28, PCB-52, PCB-77, and PCB-126, the solubility of PCB-1, PCB-3, PCB-4, and PCB-8 were relatively larger. Therefore, salting-out effect (concentration of NaCl) was the major influencing factor with respect to PCB-1, PCB-3, PCB-4, and PCB-8. From the result of RSM, the software summarized the optimum concentration of NaCl and temperature to be 11.3% (w/v) and 33.0 °C, respectively, with the maximum adsorbed amounts of 1.66, 1.79, 1.84, 1.90 and 1.97 mg/g for PCB-1, PCB-3, PCB-4, PCB-8 and PCB-28, respectively. What is more, the maximum adsorbed amounts of PCB-52, PCB-77, PCB-126, PCB-138, PCB-180 are 2.00 mg/g.

3.2.3. Desorption conditions

It is important to desorb the analytes completely from the V-g-C₃N₄/Fe₃O₄ nanoparticles for subsequent HPLC analysis. The organic solvent used as eluent directly affects the extraction efficiency and the MSPE procedure. Considering that HPLC was used to determine the PCBs, liquid desorption was employed in this

work, and various desorption solvent such as methanol, ethanol, acetone and acetonitrile were studied. A 1.0 mg of V-g-C₃N₄/Fe₃O₄ nanocomposites was used to extract the analytes from 1.0 mL of spiked water samples (concentration: 2.0 $\mu\text{g/mL}$). As shown in Fig. S5, ethanol exhibited better desorption efficiency for the target PCBs than that of the others because of its suitable polarity, and it sufficiently inhibited the interactions to provide the highest stripping efficiency. Hence, ethanol was selected as the washing solvent for the MSPE procedure.

3.2.4. Optimization of MSPE

Although a very small amount of sorbent was needed in the adsorption of trace PCBs (0.05 $\mu\text{g/mL}$) in water samples (50 mL) according to the theoretical adsorption capacity of V-g-C₃N₄/Fe₃O₄, a larger amount of sorbent was required to achieve facile phase separation and to get a higher recovery. Therefore, the amount of the sorbent V-g-C₃N₄/Fe₃O₄ in the range of 1–15 mg on the adsorption efficiency of PCBs was investigated to determine the optimum value for MSPE. The recoveries increased with the increase of sorbent from 1.0 to 10.0 mg, and then stabilized with further increase. With the increasing sorbent from 10.0 to 15.0 mg, the elution times increase. Thus, this result demonstrated that 10.0 mg of the sorbent was sufficient to extract PCBs.

Because the amount of ethanol affects the elution efficiency, the eluent volume was optimized. The recoveries increased with increasing eluent volume when the volume of the elution solvent was in the range of 0.5–1.0 mL. However, when it was from 2.0 to 4.0 mL, the recoveries decreased. Therefore, 1.0 mL wash with ethanol were selected for elution.

3.3. Analytical performance

The analytical performance of V-g-C₃N₄/Fe₃O₄-GC-MS was evaluated under the optimized conditions (sample volume, 50 mL; extraction time, 30 s; 11.3% NaCl, no pH adjustment; desorption solvent, 1 mL of ethanol; desorption time, 1 min) The name of the ten PCBs, the selected SIM ions and the retention times under the given experimental conditions are listed in Table S6. The limits

Table 2
Comparison of different methods for extraction of PCBs.

Methods	Species of PCBs	Evaluated sample	Amount of sorbent (mg)	Sample volume (mL)	Extraction time	LODs ($\mu\text{g/mL}$)	RSDs (%)	Recovery (%)	Ref.
MWCNTs-COO-/PDDA@Fe ₃ O ₄ -MPSE-GC-MS	28,52,101, 138,153,180	Water	50	500	30 min	3.1×10^{-5} – 6.9×10^{-5}	3.8–9.4	71.7–98.9	[55]
Fe ₃ O ₄ @CONPs-MSPE-GC-MS	28,52,101, 138,153,180	Water	50	200	65 min	2.7×10^{-5} – 5.9×10^{-5}	–	77.2–99.7	[56]
Fe ⁰ /iron oxide-oxyhydroxide/graphene-MSPE-GC-MS	28,52,101,138, 153,180,209	Water	15	50	20 min	–	<7	90–93	[57]
PA-Fe ₃ O ₄ NPs-MSPE-GC-MS	28,52,101,118, 138,153,180	Water, soil leachate	150–250	50	30 min	2.01×10^{-5} – 4.75×10^{-5}	<9	86–109	[28]
PDMS-SBSE-TD-GC-MS/MS	8,20,28,35,52, 101,118,138, 153,180	Water	–	200	24h	3.0×10^{-6}	<30	74–111	[58]
PDMS-SBSE-TD-GC-MS	28,52,138, 153,180	Marine water	–	10	14h	5.0×10^{-6} – 1.5×10^{-5}	<20	20–90	[59]
PANI/OH-MWCNTs-SBSE-HPLC-UV	28,52,101	Water and sediment	–	10	50 min	9.0×10^{-5} – 4.0×10^{-4}	7.0–15.4	80–121.3	[60]
PANI/ α -CD-SBSE-HPLC-UV	28,52,101,118, 138,153,180	Water	–	10	50 min	4.8×10^{-5} – 2.2×10^{-4}	5.3–9.8	82.7–121	[32]
V-g-C ₃ N ₄ /Fe ₃ O ₄ -MSPE-HPLC-UV	1,3,4,8,28,52, 77,126,138,180	Water	10	50	30s	9.0×10^{-6} – 5.8×10^{-5}	0.02–3.7	80.1–118.4	This work

of detection (LODs) of the proposed method were determined by analysis of five replicates of extracts obtained from water, which were calculated based on $S/N=3$, and ranged from 9.0×10^{-6} to $5.8 \times 10^{-5} \mu\text{g/mL}$. A good linearity was obtained in a concentration range of 5.0×10^{-4} – $0.1 \mu\text{g/mL}$ for the analytes, with determination coefficients (R^2) of 0.9850–0.9985, 0.9847–0.9982, 0.9847–0.9984, 0.9825–0.9980 for Tap water, Qingren Lake, Yangtze River and Waste water, respectively (Table S7). The results indicated that the matrix effect did not affect the quantification of the method. United States Environmental Protection Agency (USEPA) risk assessments indicate that the concentration of the drinking water standards and health advisories representing a $5.0 \times 10^{-4} \mu\text{g/mL}$ cancer risk level for some PCBs. Thus, the developed method had a good linear range, low LOD, and high reproducibility.

As is shown in Table 2, the comparison of the MSPE method with different extraction methods for the determination of PCBs was summarized. Among the reported methods for PCBs' analysis, the synthetic nanocomposites presented faster extraction kinetics (30 s) and desorption kinetics (<1 min). In addition, the present method required smaller amounts of the sorbent (10 mg) and less volume (3–4 mL), and easy to operate.

3.4. Real samples analysis

Finally, real water samples from Tap water, Qingren Lake, Yangtze River and Waste water (the water qualities were shown in Table S8) in Nanjing, Jiangsu, China, were collected and analyzed to demonstrate the extraction performance and potential application of the developed MSPE method. As can be seen, none of target analytes was detected in the Tap water, Qingren Lake, and Yangtze River samples. However, PCB-77 ($2.5 \times 10^{-3} \mu\text{g/mL}$) and PCB-126 ($3.2 \times 10^{-3} \mu\text{g/mL}$) were detected in the Waste water. The water samples ($0.003 \mu\text{g/mL}$, $0.02 \mu\text{g/mL}$ and $0.05 \mu\text{g/mL}$, 50 mL ($n=3$)) were spiked and analyzed under optimal conditions, and the recoveries obtained in the determination of PCBs are as shown in Table S9. All of the recoveries were in the range of 80.1–118.4% with relative standard deviations (RSDs) between 0.02 and 3.7%. As is shown in Fig. 4, Waste water, Waste water after MSPE, the spiked sample with standards ($c=0.003 \mu\text{g/mL}$) and the spiked sample with standards ($c=0.003 \mu\text{g/mL}$) after MSPE were determined by GC-MS, and clear chromatographic peaks of PCBs were observed after MSPE. In conclusion, V-g-C₃N₄/Fe₃O₄ has the potential application prospect in the analysis of nonpolar carbon-based ring compounds in water samples.

3.5. Reusability of V-g-C₃N₄/Fe₃O₄

The magnetic nanocomposites were reused in MSPE to investigate the recyclability of the sorbent. There was no obvious decrease or increase in the analyte recoveries after five times of reuse. The recoveries of PCBs were 85.4–93.4% for PCB-1, 99.1–105.0% for PCB-3, 96.0–99.3% for PCB-4, 99.0–102.4% for PCB-8, 98.5–101.4% for PCB-28, 97.7–103.4% for PCB-52, 99.3–103.5% for PCB-77, 99.6–102.2% for PCB-126, 96.8–99.4% for PCB-138, 97.8–99.2% for PCB-180. The results indicate that V-g-C₃N₄/Fe₃O₄ is stable and no carryover of PCBs occurred during the MSPE procedure, indicating good reusability.

4. Conclusion

In this work, a new V-g-C₃N₄/Fe₃O₄ nanocomposite was synthesized by chemical co-precipitation. The experimental strategy was environmental friendly. The magnetic material was evaluated in terms of the adsorption and desorption of ten PCBs. The MSPE conditions were optimized using RSM, and applied to

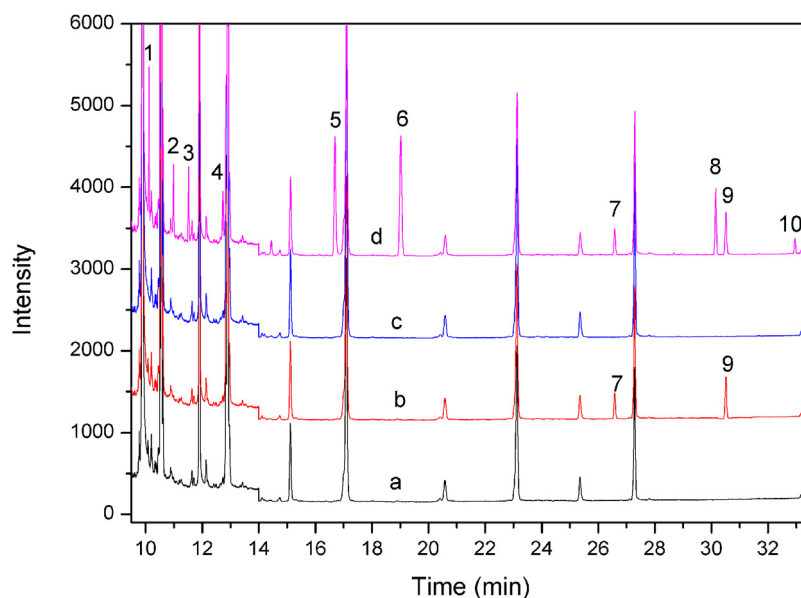


Fig. 4. GC–MS chromatograms of target PCBs in (a) Waste water; (b) Waste water obtained after MSPE; (c) spiked sample with standards ($c = 0.003 \mu\text{g/mL}$); (d) spiked sample with standard after MSPE ($c = 0.003 \mu\text{g/mL}$). Peaks of 1–10 represent PCB-1, PCB-3, PCB-4, PCB-8, PCB-28, PCB-77, PCB-138, PCB-126 and PCB-180, respectively.

the pre-concentration of PCBs in water samples. The nanocomposite showed high extraction efficiency for targeted analytes due to hydrophobic effect, π – π conjugate function and inclusion effect between porous V-g- $\text{C}_3\text{N}_4/\text{Fe}_3\text{O}_4$ and the targeted PCBs. The nanocomposites with a large surface area have the advantages of quick adsorption (30 s) and is reusable. It was used to develop a highly sensitive magnetic solid-phase extraction method. Good linearity, recovery and low limits of detection were demonstrated, indicating that V-g- $\text{C}_3\text{N}_4/\text{Fe}_3\text{O}_4$ can be used in the pretreatment and removal of PCBs from water samples, as well as other environmental nonpolar pollutants which contained carbon-based ring structures.

Acknowledgements

This research was supported by the National Natural Science Foundation of China (Grant No. 21475061 and 21507062), the Scientific Research Foundation for the Returned Overseas Chinese Scholars, State Education Ministry ([2015]1098), Program of Natural Science Research of Jiangsu Higher Education Institutions of China (Grant No. 16KJB150022), the Priority Academic Program Development of Jiangsu Higher Education Institutions, Jiangsu Collaborative Innovation Center of Biomedical Functional Materials, and Chinese National Scholarship for Graduate Students (Man Wang).

Appendix A. Supplementary data

Supplementary data associated with this article can be found, in the online version, at <http://dx.doi.org/10.1016/j.chroma.2017.02.048>.

References

- [1] A. Azzouz, E. Ballesteros, Trace analysis of endocrine disrupting compounds in environmental water samples by use of solid-phase extraction and gas chromatography with mass spectrometry detection, *J. Chromatogr. A* 1360 (2014) 248–257.
- [2] M. Gorga, M. Petrovic, D. Barcelo, Multi-residue analytical method for the determination of endocrine disruptors and related compounds in river and waste water using dual column liquid chromatography switching system coupled to mass spectrometry, *J. Chromatogr. A* 1295 (2013) 57–66.
- [3] X.-T. Peng, L. Jiang, Y. Gong, X.-Z. Hu, L.-J. Peng, Y.-Q. Feng, Preparation of mesoporous ZrO_2 -coated magnetic microsphere and its application in the multi-residue analysis of pesticides and PCBs in fish by GC–MS/MS, *Talanta* 132 (2015) 118–125.
- [4] N. Khodae, A. Mehdinia, R. Esfandiarnajad, A. Jabbari, Ultra trace analysis of PAHs by designing simple injection of large amounts of analytes through the sample reconcentration on SPME fiber after magnetic solid phase extraction, *Talanta* 147 (2016) 59–62.
- [5] M. Locatelli, F. Sciascia, R. Cifelli, L. Malatesta, P. Bruni, F. Croce, Analytical methods for the endocrine disruptor compounds determination in environmental water samples, *J. Chromatogr. A* 1434 (2016) 1–18.
- [6] S. Ozcan, Analyses of polychlorinated biphenyls in waters and wastewaters using vortex-assisted liquid–liquid microextraction and gas chromatography–mass spectrometry, *J. Sep. Sci.* 34 (2011) 574–584.
- [7] R. Westbom, L. Thörneby, S. Zorita, L. Mathiasson, E. Björklund, Development of a solid-phase extraction method for the determination of polychlorinated biphenyls in water, *J. Chromatogr. A* 1033 (2004) 1–8.
- [8] L. Han, Y. Sapozhnikova, S.J. Lehotay, Streamlined sample cleanup using combined dispersive solid-phase extraction and in-vial filtration for analysis of pesticides and environmental pollutants in shrimp, *Anal. Chim. Acta* 827 (2014) 40–46.
- [9] A.V. de Baires, R.M. de Almeida, L. Pantaleao, T. Barcellos, S. Moura e Silva, M. Yonamine, Determination of low levels of benzodiazepines and their metabolites in urine by hollow-fiber liquid-phase microextraction (LPME) and gas chromatography–mass spectrometry (GC–MS), *J. Chromatogr. B* 975 (2015) 24–33.
- [10] O. Krueger, S. Olberg, R. Senz, F.-G. Simon, Comparison of stir bar sorptive extraction (SBSE) and solid phase microextraction (SPME) for the analysis of polycyclic aromatic hydrocarbons (PAH) in complex aqueous soil leachates, *Water, Air, Soil. Pollut.* 226 (2015).
- [11] F. Zhu, J. Wang, L. Zhu, L. Tan, G. Feng, S. Liu, Y. Dai, H. Wang, Preparation of molecularly imprinted polymers using theanine as dummy template and its application as SPE sorbent for the determination of eighteen amino acids in tobacco, *Talanta* 150 (2016) 388–398.
- [12] F. Li, J. Jin, D. Tan, J. Xu, Y. Dhanjai, H. Ni, J. Zhang, Chen, High performance solid-phase extraction cleanup method coupled with gas chromatography–triple quadrupole mass spectrometry for analysis of polychlorinated naphthalenes and dioxin-like polychlorinated biphenyls in complex samples, *J. Chromatogr. A* 2016 (1448) 1–8.
- [13] J.J. Ramos, B. Gomara, M.A. Fernandez, M.J. Gonzalez, A simple and fast method for the simultaneous determination of polychlorinated biphenyls and polybrominated diphenyl ethers in small volumes of human serum, *J. Chromatogr. A* 1152 (2007) 124–129.
- [14] D. Lu, Y. Lin, C. Feng, D. Wang, X. Qiu, Y. e. Jin, L. Xiong, Y. Jin, G. Wang, Determination of polybrominated diphenyl ethers and polychlorinated biphenyls in fishery and aquaculture products using sequential solid phase extraction and large volume injection gas chromatography/tandem mass spectrometry, *J. Chromatogr. B* 945–946 (2014) 75–83.
- [15] Z. Zhang, S.M. Rhind, Optimized determination of polybrominated diphenyl ethers and polychlorinated biphenyls in sheep serum by solid-phase extraction–gas chromatography–mass spectrometry, *Talanta* 84 (2011) 487–493.
- [16] W. Guan, Z. Long, J. Liu, Y. Hua, Y. Ma, H. Zhang, Unique graphitic carbon nitride nanovessels as recyclable adsorbent for solid phase extraction of

- benzoylurea pesticides in juices samples, *Food. Anal. Methods* 8 (2015) 2202–2210.
- [17] J. Nasiri, M.R. Naghavi, H. Alizadeh, M.R.F. Moghadam, E. Motamedi, A. Mashouf, Magnetic solid phase extraction coupled with HPLC towards removal of pigments and impurities from leaf-derived paclitaxel extractions of *taxus baccata* and optimization via response surface methodology, *Chromatographia* 78 (2015) 1143–1157.
- [18] J. Yang, L. Si, S. Cui, W. Bi, Synthesis of a graphitic carbon nitride nanocomposite with magnetite as a sorbent for solid phase extraction of phenolic acids, *Microchim. Acta* 182 (2015) 737–744.
- [19] T. Sano, S. Tsutsui, K. Koike, T. Hirakawa, Y. Teramoto, N. Negishi, K. Takeuchi, Activation of graphitic carbon nitride ($g\text{-C}_3\text{N}_4$) by alkaline hydrothermal treatment for photocatalytic NO oxidation in gas phase, *J. Mater. Chem. A* 1 (2013) 6489–6496.
- [20] X.Y. Yuan, C. Zhou, Y.R. Jin, Q.Y. Jing, Y.L. Yang, X. Shen, Q. Tang, Y.H. Mu, A.K. Du, Facile synthesis of 3D porous thermally exfoliated $g\text{-C}_3\text{N}_4$ nanosheet with enhanced photocatalytic degradation of organic dye, *J. Colloid Interface Sci.* 468 (2016) 211–219.
- [21] Z.Y. Wang, W. Guan, Y.J. Sun, F. Dong, Y. Zhou, W.K. Ho, Water-assisted production of honeycomb-like $g\text{-C}_3\text{N}_4$ with ultralong carrier lifetime and outstanding photocatalytic activity, *Nanoscale* 7 (2015) 2471–2479.
- [22] Y. -p. Sun, W. Ha, J. Chen, H. -y. Qi, Y. -p. Shi, Advances and applications of graphitic carbon nitride as sorbent in analytical chemistry for sample pretreatment: a review, *Trends Anal. Chem.* 84 (2016) 12–21.
- [23] M. Wang, S. Cui, X. Yang, W. Bi, Synthesis of $g\text{-C}_3\text{N}_4/\text{Fe}_3\text{O}_4$ nanocomposites and application as a new sorbent for solid phase extraction of polycyclic aromatic hydrocarbons in water samples, *Talanta* 132 (2015) 922–928.
- [24] A.L. Daniel-da-Silva, A.M. Salgueiro, B. Creaney, R. Oliveira-Silva, N.J.O. Silva, T. Trindade, Carrageenan-grafted magnetite nanoparticles as recyclable sorbents for dye removal, *J. Nanopart. Res.* 17 (2015) 15.
- [25] Y. Pan, N. Li, J.S. Mu, R.H. Zhou, Y. Xu, D.Z. Cui, Y. Wang, M. Zhao, Biogenic magnetic nanoparticles from *Burkholderia* sp. YN01 exhibiting intrinsic peroxidase-like activity and their applications, *Appl. Microbiol. Biotechnol.* 99 (2015) 703–715.
- [26] A. Sergi, F. Shemirani, M. Alvand, A. Tajbakhshian, Graphene oxide magnetic nanocomposites for the preconcentration of trace amounts of malachite green from fish and water samples prior to determination by fiber optic-linear array detection spectrophotometry, *Anal. Methods* 6 (2014) 7744–7751.
- [27] G. Ctistis, P. Schon, W. Bakker, G. Luthe, PCDDs PCDFs, and PCBs co-occurrence in TiO_2 nanoparticles, *Environ. Sci. Pollut. Res.* 23 (2016) 4837–4843.
- [28] R.A. Perez, B. Albero, J.L. Tadeo, E. Molero, C. Sanchez-Brunete, Application of magnetic iron oxide nanoparticles for the analysis of PCBs in water and soil leachates by gas chromatography-tandem mass spectrometry, *Anal. Bioanal. Chem.* 407 (2015) 1913–1924.
- [29] P. Tremolada, N. Guazzoni, R. Comolli, M. Parolini, S. Lazzaro, A. Binelli, Polychlorinated biphenyls (PCBs) in air and soil from a high-altitude pasture in the Italian Alps: evidence of CB-209 contamination, *Environ. Sci. Pollut. Res.* 22 (2015) 19571–19583.
- [30] U. Berger, D. Herzke, T.M. Sandanger, Two trace analytical methods for determination of hydroxylated PCBs and other halogenated phenolic compounds in eggs from Norwegian birds of prey, *Anal. Chem.* 76 (2004) 441–452.
- [31] S.G. Chu, C.S. Hong, B.A. Rattner, P.C. McGowan, Methodological refinements in the determination of 146 polychlorinated biphenyls including non-ortho- and mono-ortho-substituted PCBs, and 26 organochlorine pesticides as demonstrated in heron eggs, *Anal. Chem.* 75 (2003) 1058–1066.
- [32] Y. Lei, M. He, B. Chen, B. Hu, Polyaniline/cyclodextrin composite coated stir bar sorptive extraction combined with high performance liquid chromatography-ultraviolet detection for the analysis of trace polychlorinated biphenyls in environmental waters, *Talanta* 150 (2016) 310–318.
- [33] A. Perrard, C. Descorme, Static and dynamic adsorption studies of PolyChloroBiphenyls (PCBs) over activated carbons, *Chemosphere* 145 (2016) 528–534.
- [34] S. Centi, E. Silva, S. Laschi, I. Palchetti, M. Mascini, Polychlorinated biphenyls (PCBs) detection in milk samples by an electrochemical magneto-immunosensor (EMI) coupled to solid-phase extraction (SPE) and disposable low-density arrays, *Anal. Chim. Acta* 594 (2007) 9–16.
- [35] S. Fu, J. Zhang, T. Li, S. Wang, W.J. Ding, M.M. Zhao, Y.F. Du, Q. Wang, J. Jia, Multi-responses extraction optimization based on response surface methodology combined with polarity switching HPLC MS/MS for the simultaneous quantitation of 11 compounds in Cortex Fraxini: application to four species of Cortex Fraxini and its 3 confusable species, *J. Pharm. Biomed. Anal.* 91 (2014) 210–221.
- [36] A.O. Beringhs, M. Dalmina, T.B. Creczynski-Pasa, D. Sonaglio, Response Surface Methodology IV-Optimal design applied to the performance improvement of an RP-HPLC-UV method for the quantification of phenolic acids in *Cecropia glaziovii* products, *Rev. Bras. Farmacogn.-Braz. J. Pharmacogn.* 25 (2015) 513–521.
- [37] F.J. Li, S.L. Ning, Y. Li, Y.J. Yu, C.D. Shen, G.L. Duan, Optimisation of infrared-assisted extraction of rutin from crude flos sophorae immaturus using response surface methodology and HPLC analysis, *Phytochem. Anal.* 23 (2012) 292–298.
- [38] S.L.C. Ferreira, R.E. Bruns, H.S. Ferreira, G.D. Matos, J.M. David, G.C. Brandao, E.G.P. da Silva, L.A. Portugal, P.S. Reis, A.S. Souza, W.N.L. dos Santos, Box-Behnken design: an alternative for the optimization of analytical methods, *Anal. Chim. Acta* 597 (2007) 179–186.
- [39] C.L. Ye, C.J. Jiang, Optimization of extraction process of crude polysaccharides from *Plantago asiatica* L. by response surface methodology, *Carbohydr. Polym.* 84 (2011) 495–502.
- [40] A. Stafiej, K. Pyrzynska, A. Ranz, E. Lankmayr, Screening and optimization of derivatization in heating block for the determination of aliphatic aldehydes by HPLC, *J. Biochem. Biophys. Methods* 69 (2006) 15–24.
- [41] H. Liu, X.L. Du, Q.P. Yuan, L. Zhu, Optimisation of enzyme assisted extraction of silybin from the seeds of *Silybum marianum* by Box-Behnken experimental design phytochem, *Anal* 20 (2009) 475–483.
- [42] W.T. Bi, M.L. Tian, K.H. Row, Evaluation of alcohol-based deep eutectic solvent in extraction and determination of flavonoids with response surface methodology optimization, *J. Chromatogr. A* 1285 (2013) 22–30.
- [43] G.N. Rallis, V.A. Sakkas, V.A. Boumba, T. Vougiouklakis, T.A. Albanis, Determination of organochlorine pesticides and polychlorinated biphenyls in post-mortem human lung by matrix solid-phase dispersion with the aid of response surface methodology and desirability function, *J. Chromatogr. A* 1227 (2012) 1–9.
- [44] L. Liu, Y.-B. Wen, K.-N. Liu, L. Sun, M. Wu, G.-F. Han, Y.-X. Lu, Q.-M. Wang, Z. Yin, Optimization of on-line solid phase extraction and HPLC conditions using response surface methodology for determination of WM-5 in mouse plasma and its application to pharmacokinetic study, *J. Chromatogr. B Analyt. Technol. Biomed. Life. Sci.* 923 (2013) 8–15.
- [45] Y.-K. Liu, X.-Y. Jia, X. Liu, Z.-Q. Zhang, On-line solid-phase extraction-HPLC-fluorescence detection for simultaneous determination of puerarin and daidzein in human serum, *Talanta* 82 (2010) 1212–1217.
- [46] D.J. Silva, F.V. Pietri, J.E.F. Moraes, R.C. Bazito, C.G. Pereira, Treatment of materials contaminated with polychlorinated biphenyls (PCBs): comparison of traditional method and supercritical fluid extraction, *Am. J. Anal. Chem.* 3 (2012) 891–898.
- [47] Y. Xu, M. Xie, S. Huang, H. Xu, H. Ji, J. Xia, Y. Li, H. Li, High yield synthesis of nano-size $g\text{-C}_3\text{N}_4$ derivatives by a dissolve-regrowth method with enhanced photocatalytic ability, *RSC Adv.* 5 (2015) 26281–26290.
- [48] J.Y. Qin, J.P. Huo, P.Y. Zhang, J. Zeng, T.T. Wang, H.P. Zeng, Improving the photocatalytic hydrogen production of $\text{Ag}/g\text{-C}_3\text{N}_4$ nanocomposites by dye-sensitization under visible light irradiation, *Nanoscale* 8 (2016) 2249–2259.
- [49] D.X. Yang, T. Jiang, T.B. Wu, P. Zhang, H.L. Han, B.X. Han, Highly selective oxidation of cyclohexene to 2-cyclohexene-1-one in water using molecular oxygen over Fe-Co- $g\text{-C}_3\text{N}_4$, *Catal. Sci. Technol.* 6 (2016) 193–200.
- [50] M. Mousavi, A. Habibi-Yangjeh, Magnetically separable ternary $g\text{-C}_3\text{N}_4/\text{Fe}_3\text{O}_4/\text{BiOI}$ nanocomposites: novel visible-light-driven photocatalysts based on graphitic carbon nitride, *J. Colloid Interface Sci.* 465 (2016) 83–92.
- [51] G. Liu, X. Yang, T. Li, Y. She, S. Wang, J. Wang, M. Zhang, F. Jin, M. Jin, H. Shao, M. Shi, Preparation of a magnetic molecularly imprinted polymer using $g\text{-C}_3\text{N}_4/\text{Fe}_3\text{O}_4$ for atrazine adsorption, *Mater. Lett.* 160 (2015) 472–475.
- [52] W. Bi, J. Zhou, K.H. Row, Solid phase extraction of lactic acid from fermentation broth by anion-exchangeable silica confined ionic liquids, *Talanta* 83 (2011) 974–979.
- [53] W. Bi, J. Zhou, K.H. Row, Separation of xylose and glucose on different silica-confined ionic liquid stationary phases, *Anal. Chim. Acta* 677 (2010) 162–168.
- [54] Y. Jin, D.K. Choi, K.H. Row, Adsorption isotherms of caffeine on molecular imprinted polymer, *Kor. J. Chem. Eng.* 25 (2008) 816–818.
- [55] S. Zeng, Y. Cao, W. Sang, T. Li, N. Gan, L. Zheng, Enrichment of polychlorinated biphenyls from aqueous solutions using Fe_3O_4 grafted multiwalled carbon nanotubes with poly dimethyl diallyl ammonium chloride, *Int. J. Mol. Sci.* 13 (2012) 6382–6398.
- [56] S. Zeng, N. Gan, R. Weideman-Mera, Y. Cao, T. Li, W. Sang, Enrichment of polychlorinated biphenyl 28 from aqueous solutions using Fe_3O_4 grafted graphene oxide, *Chem. Eng. J.* 218 (2013) 108–115.
- [57] A.A. Karamani, A.P. Douvalis, C.D. Stalikas, Zero-valent iron/iron oxide-oxyhydroxide/graphene as a magnetic sorbent for the enrichment of polychlorinated biphenyls, polyaromatic hydrocarbons and phthalates prior to gas chromatography-mass spectrometry, *J. Chromatogr. A* 1271 (2013) 1–9.
- [58] F.J. Camino-Sanchez, A. Zafrá-Gomez, S. Cantarero-Malagon, J.L. Vilchez, Validation of a method for the analysis of 77 priority persistent organic pollutants in river water by stir bar sorptive extraction in compliance with the European Water Framework Directive, *Talanta* 89 (2012) 322–334.
- [59] E. Perez-Carrera, V.M.L. Leon, A.G. Parra, E. Gonzalez-Mazo, Simultaneous determination of pesticides polycyclic aromatic hydrocarbons and polychlorinated biphenyls in seawater and interstitial marine water samples, using stir bar sorptive extraction-thermal desorption-gas chromatography-mass spectrometry, *J. Chromatogr. A* 1170 (2007) 82–90.
- [60] C. Hu, M. He, B. Chen, B. Hu, Simultaneous determination of polar and apolar compounds in environmental samples by a polyaniline/hydroxyl multi-walled carbon nanotubes composite-coated stir bar sorptive extraction coupled with high performance liquid chromatography, *J. Chromatogr. A* 1394 (2015) 36–45.